Available online at www.sciencedirect.com
SCIENCE DIRECT®
Journal of Nuclear Materials 322 (2003) 217–227
journal of nuclear materials
www.elsevier.com/locate/jnucmat

Tensile behaviour and acoustic emission in zirconium alloys after thermal aging and sodium exposure

P.K. Chaurasia, C.K. Mukhopadhyay, S. Murugan, P. Muralidharan, K. Chandran, V. Ganesan, T. Jayakumar *, P.V. Kumar

Materials, Chemical and Reprocessing Groups, Indira Gandhi Centre for Atomic Research, Kalpakkam 603102, Tamil Nadu, India

Received 17 March 2003; accepted 18 July 2003

Abstract

Tubular specimens of Zircaloy-2 and Zr–2.5%Nb alloys were exposed to flowing sodium at 613 K for different durations. Similar tubular specimens of the two alloys were also given equivalent thermal treatment. Tensile testing of all the specimens was carried out at a nominal strain rate of 5×10^{-4} s^{-1} and ambient temperature (298 K) along with recording of acoustic emission (AE) signals. Microhardness values of the specimens were determined. The tensile and microhardness results indicated marginal changes in the properties consequent to sodium exposure and thermal treatment. Higher AE generated in the sodium exposed and thermally treated specimens as compared to non-exposed/heat-treated specimens is attributed to decohesion of hydride platelets during tensile testing. While the tensile properties could not show any difference between the untreated and treated specimens, the AE results could very well bring out higher amount of decohesion of hydrides in sodium exposed as compared to thermally aged specimens.

1. Introduction

Zirconium alloys are extensively used in thermal reactors as they have low neutron absorption cross sections, acceptable corrosion resistance to hot pressurized water and good mechanical properties in the operating temperature regimes of thermal reactors. An experiment was carried out to determine the in-reactor creep rate of indigenously developed zirconium alloys used in the Indian pressurized heavy water reactors (PHWRs) by irradiating these materials in the fast breeder test reactor (FBTR). Testing of materials in a fast reactor reduces the time required to achieve a desired radiation damage level, due to higher neutron flux and harder spectrum of fast reactors. Irradiation of zirconium alloys in FBTR requires that the compatibility of zirconium alloys with sodium, which is used as coolant in FBTR, be established at the test temperatures of around 573 K. It is reported in the literature that zirconium alloys have good compatibility with sodium up to 873 K [1]. However, there are not many detailed studies carried out to determine the changes in the mechanical properties of zirconium alloys owing to their exposure to sodium. The objective of the present investigation is to study the effect of exposure to sodium on mechanical properties of these alloys. This has been done by comparing the changes in the mechanical properties of these alloys due to exposure to high temperature reactor grade sodium at 613 K to those due to equivalent thermal treatment.

Acoustic emission (AE) generated during tensile deformation of a material is strongly influenced by the changes in the microstructures and the associated changes in the tensile deformation and fracture. In view of this, AE monitoring during tensile testing of different specimens exposed to sodium and thermal aging was done and analyzed to gain an insight into changes in deformation behaviour in different specimens.

* Corresponding author. Tel.: +91-4114 280208; fax: +91-4114 280356.
E-mail address: tjk@igcar.ernet.in (T. Jayakumar).

0022-3115/$ - see front matter © 2003 Elsevier B.V. All rights reserved.
doi:10.1016/S0022-3115(03)00329-5

AE is the phenomenon whereby transient elastic waves are generated by rapid release of energy from localised sources in a material [2]. A transducer or sensor acoustically coupled to a sample detects the elastic (acoustic) energy emitted by the sample and gives information about the dynamic changes taking place in the sample. The acoustic emission technique (AET) is extensively used for studying the deformation and fracture behaviour in materials [2]. The extent of the acoustic activity generated during deformation of a material depends on a number of factors such as type of material and its metallurgical history, level of plastic strain and presence of any inclusions or second phase. AE generated during tensile deformation of metallic materials indicated that for materials having a single-phase microstructure, a peak in AE occurs at initial strain levels corresponding to the phenomenon of macroyielding [3,4]. Studies on AE generated during the deformation of zirconium alloys have been reported in the literature [4–6]. It is known from these investigations that both slip and twinning give rise to AE during deformation of these alloys. With increasing strain level, AE due to both these phenomena is reduced.

In the present investigation, in addition to AE, hardness measurements, metallographic and scanning electron microscopic (SEM) examinations were carried out to understand and explain the observed changes in mechanical properties and AE due to sodium exposure and thermal treatment.

2. Materials

The materials used in the present investigation (Zircaloy-2 and Zr–2.5%Nb alloy) were obtained in the hot-extruded and cold-pilgered conditions. Following β-quenching treatment, tubes of Zircaloy-2 were hot-extruded (extrusion ratio 6.9) and pilgered in two passes (59.2% and 24% cold work in the first pass and second pass). Similarly, tubes of Zr–2.5%Nb alloy, after β-quenching, were hot-extruded (extrusion ratio 6.9) and pilgered in two passes (55% and 22.4% cold work in the first pass and second pass). The chemical composition of Zircaloy-2 and Zr–2.5%Nb alloy is given in Table 1. In the as-received condition, the average grain size of Zircaloy-2 is approximately 8 μm and that of Zr–2.5%Nb alloy is less than 1 μm.

3. Experimental

Tubular tensile specimens in accordance with ASTM specification E8 and E453 were made from Zircaloy-2 and Zr–2.5%Nb alloy tubes. The outer diameter of the specimens is 15.3 mm and the nominal wall thickness is 0.65 mm. The length of the specimen is chosen to be 180 mm.

An experimental loop was fabricated for carrying out the sodium–zirconium alloys compatibility experiments (Fig. 1). The loop consists of a vessel, which was fabricated from a stainless steel (AISI type 304) pipe of 100 mm nominal diameter to hold the specimens. The specimens were arranged inside the vessel using a specimen holder such that there was no contact between the specimens, and sodium could flow freely around the specimens. The top portion of the vessel was closed with a knife-edge type high vacuum flange. Vapor separators were provided at the top portion so that the sodium vapor reaching the top portion of the vessel would condense and flow back into the vessel. A flat heater coil was wound around the vessel to maintain the temperature of sodium at 613 K. A thermowell was provided in the bottom cover plate of the vessel. A thermocouple was placed in the thermowell to measure the temperature of bulk sodium continuously. The heater current was controlled such that the sodium was maintained at the desired test temperature of 613 K during the experiments. An electromagnetic pump was used to circulate sodium in the loop. A cold-trap operating at 393 K was arranged as part of the loop to remove the impurities in the flowing sodium. The vessel and the pipes in the loop were fully insulated to reduce the heat losses. Duplicate of tubular specimens were withdrawn from the sodium loop, after every 750 h, covering a total period of 4500 h. After withdrawal, these tubes were thoroughly cleaned with alcohol to remove the sodium adhering to the surface of the specimens. Filling of sodium in the experimental loop and withdrawal of specimens were carried out inside glove boxes operating with argon atmosphere. The experiments were conducted in two batches, one batch for Zircaloy-2 specimens and another for Zr–2.5%Nb alloy specimens. Similar tubular tensile specimens of these two alloys were also separately given equivalent thermal treatments for similar durations of time. In this case, the specimens were encapsulated in quartz tubes with low pressure argon environment and aged at the temperature of 613 K in an electrical furnace.

Table 1
Chemical composition (wt%) of Zircaloy-2 and Zr–2.5%Nb alloy

Material	Fe	Cr	Ni	Sn	Nb	Mo	O	N	H
Zircaloy-2	0.07–0.20	0.05–0.15	0.03–0.08	1.2–1.7	0.01	0.005	0.14	0.01	0.0025
Zr–2.5%Nb	0.15	0.02	0.007	0.01	2.4–2.8	0.005	0.13	0.0065	0.0025

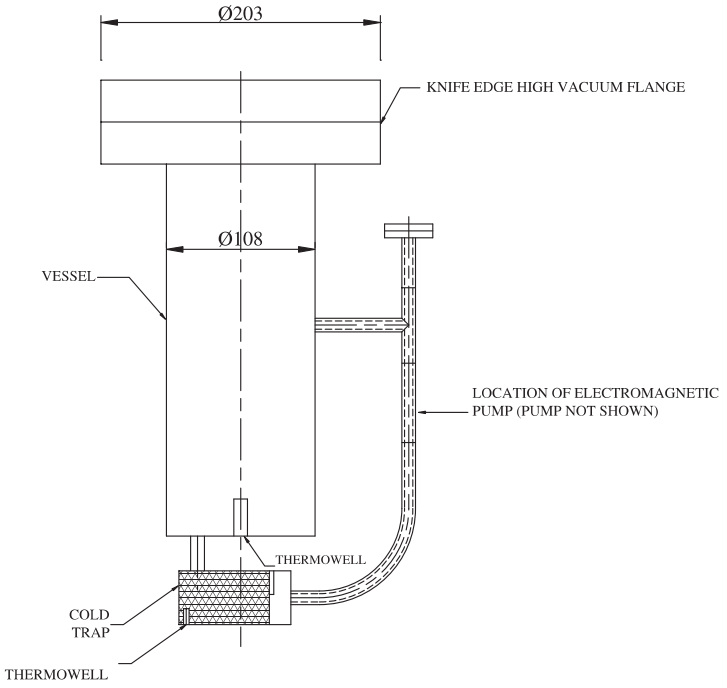

Fig. 1. Sketch of the experimental loop used for sodium–zirconium alloys compatibility experiments.

Tensile tests were carried out on all the specimens at nominal strain rate of 5×10^{-4} s^{-1} and ambient temperature (298 K) using an INSTRON 1195 tensile testing machine. The testing was carried out in accordance with the specification ASTM E253. Mandrels made of stainless steel were snugly fitted at both ends of the tubular specimens for carrying out tensile testing. The scheme of the tensile test set-up is shown in Fig. 2. AE signals generated during the tensile tests were recorded and analyzed using a Spartan 2000 acoustic emission system (M/s. Physical Acoustic Corporation, USA). A piezoelectric transducer having a resonant frequency at 150 kHz, a pre-amplifier (60 dB gain) and a compatible filter (100–300 kHz) were used (Fig. 2). A total gain of 85 dB and a threshold of 45 dB were selected so that no external noise was recorded during the experiments. This was verified by repeatedly loading and unloading a dummy specimen to load levels more than 1.5 times the maximum load required for fracture of any of the specimens used in the present study. After the first cycle, no emission was found during the subsequent loading cycles. This indicated that the AE signals were not recorded either from the machine or from any external noise, under the selected AE recording parameters.

Microhardness testing was carried out on different specimens using a LEITZ MINILOAD 2 microhardness measuring equipment (M/s. Leitz GmbH, Germany) with an indentation load of 100 g. Samples for metallographic characterisation were prepared from the tubular specimens. The etchant used was a mixture of 30 ml of 88% lactic acid, 30 ml of 69% HNO_3 and 10 ml of 40% HF. Small samples were cut from the fracture regions of the tensile tested specimens and were examined under a SEM (SEM Model XL30 ESEM of M/s. Philips, Holland).

4. Results

The optical microstructures of Zircaloy-2 and Zr–2.5%Nb alloy for as-received (unexposed) and sodium exposed (4500 h) conditions are shown in Figs. 3 and 4, respectively. The optical microstructures of the two alloys in thermally treated conditions (4500 h) are also given in Fig. 5. These figures show the presence of hydrides in the sodium exposed and thermally treated specimens as compared to the unexposed specimens of the two alloys. It is seen that most of the hydrides are aligned in the circumferential direction. Thread like morphology of the hydrides is seen. Comparison of microstructures in specimens treated for different durations indicated that the size of the hydride platelets increases with increasing time of exposure in both sodium exposed and thermally treated specimens. The number and the size of the hydride platelets are seen to be higher for the sodium exposed specimens as compared to the thermally treated specimens for equivalent duration of time.

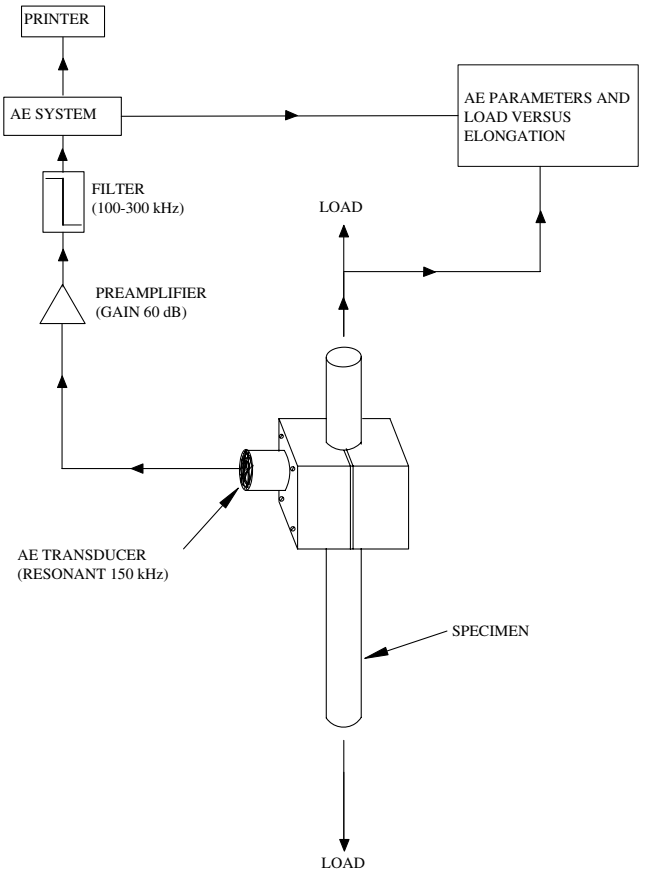

Fig. 2. Scheme of tensile test set-up.

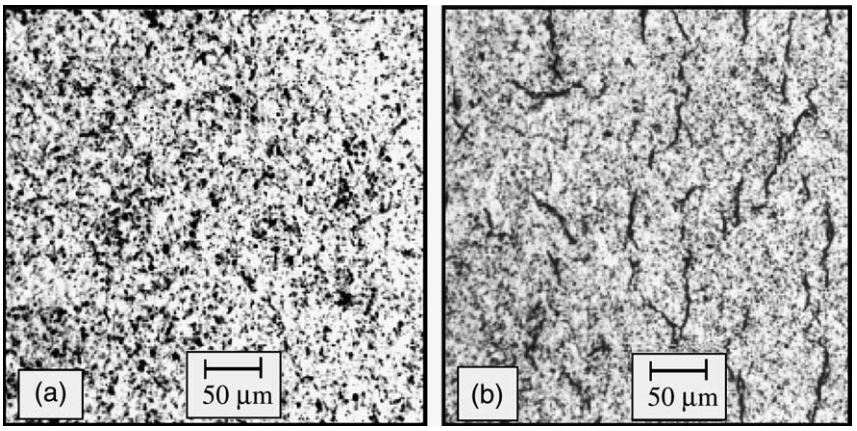

Fig. 3. Optical micrographs of Zircaloy-2: (a) unexposed condition (0 h); (b) exposed to sodium for 4500 h.

The values of yield strength, ultimate tensile strength, total elongation and microhardness of Zircaloy-2 exposed to flowing sodium at 613 K are shown in Table 2. Similar values of Zr–2.5%Nb alloy exposed to flowing sodium at 613 K are shown in Table 3. The values of strength and microhardness of thermally treated specimens of both the alloys are given in Table 4. The effect of sodium exposure on the yield strength and ultimate tensile strength of Zircaloy-2 and Zr–2.5%Nb alloy is shown in Fig. 6. The effect of sodium exposure on the

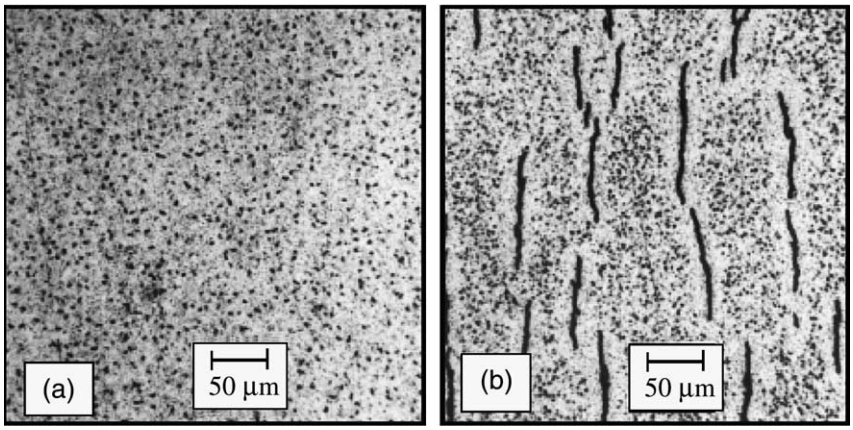

Fig. 4. Optical micrographs of Zr–2.5%Nb alloy: (a) unexposed condition (0 h); (b) exposed to sodium for 4500 h.

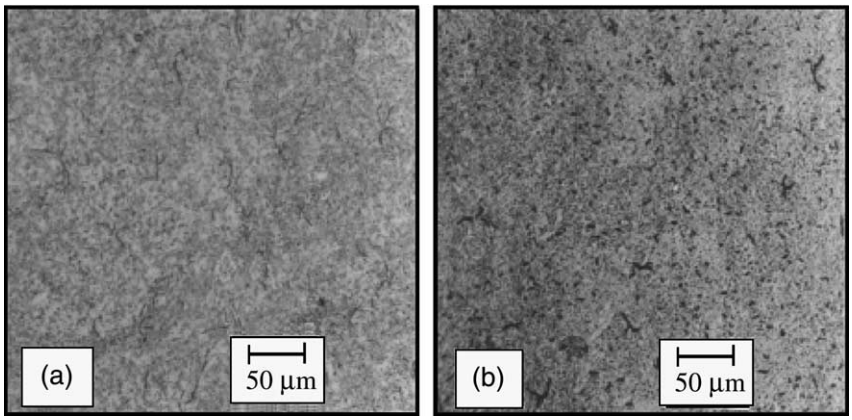

Fig. 5. Optical micrographs of thermally aged Zircaloy-2 and Zr–2.5%Nb alloy: (a) Zircaloy-2 (4500 h); (b) Zr–2.5%Nb (4500 h).

Table 2
Mechanical properties of Zircaloy-2 specimens after exposure to flowing sodium at 613 K

Duration, h	Yield strength, MPa (average)	Ultimate tensile strength, MPa (average)	Total elongation, % (average)	Microhardness, VHN (average), indentation load = 100 g
Unexposed (0 h)	462	643	20.8	252
750	424	590	16.8	248
1500	464	612	18.4	244
2250	446	632	18.2	250
3000	452	640	17.0	260
3750	455	620	19.7	242
4500	426	596	18.2	246

total elongation and microhardness of Zircaloy-2 and Zr–2.5%Nb alloy is illustrated in Fig. 7.

The tensile test results indicate that both yield strength and ultimate tensile strength of Zircaloy-2 reduce with exposure to sodium. The maximum reduction observed was 8% as compared to unexposed specimens. The total elongation was observed to lie between 16.8% and 19.7% for the exposed specimens as compared to 20.8% for unexposed specimens. In the case of Zr–2.5%Nb alloy also, the tensile test results indicate that the yield strength is reduced with exposure to sodium. The maximum reduction observed was 8% as compared

Table 3
Mechanical properties of Zr–2.5%Nb alloy specimens after exposure to flowing sodium at 613 K

Duration, h	Yield strength, MPa (average)	Ultimate tensile strength, MPa (average)	Total elongation, % (average)	Microhardness, VHN (average), indentation load = 100 g
Unexposed (0 h)	506	692	13.6	249
750	473	733	15.1	253
1500	482	739	14.0	252
2250	485	704	15.7	258
3000	465	614	20.7	250
3750	473	618	19.3	242
4500	470	613	16.7	242

Table 4
Mechanical properties of Zircaloy-2 and Zr–2.5%Nb alloy specimens after thermal aging at 613 K

Material	Duration, h	Yield strength, MPa	Ultimate tensile strength, MPa	Total elongation, %	Microhardness, VHN, indentation load = 100 g
Zircaloy-2	0	462	643	20.3	252
	2250	435	625	17.8	214
	4500	453	625	17.8	228
Zr–2.5%Nb	0	506	692	13.2	249
	2250	510	710	14.5	245
	4500	514	656	16.3	230

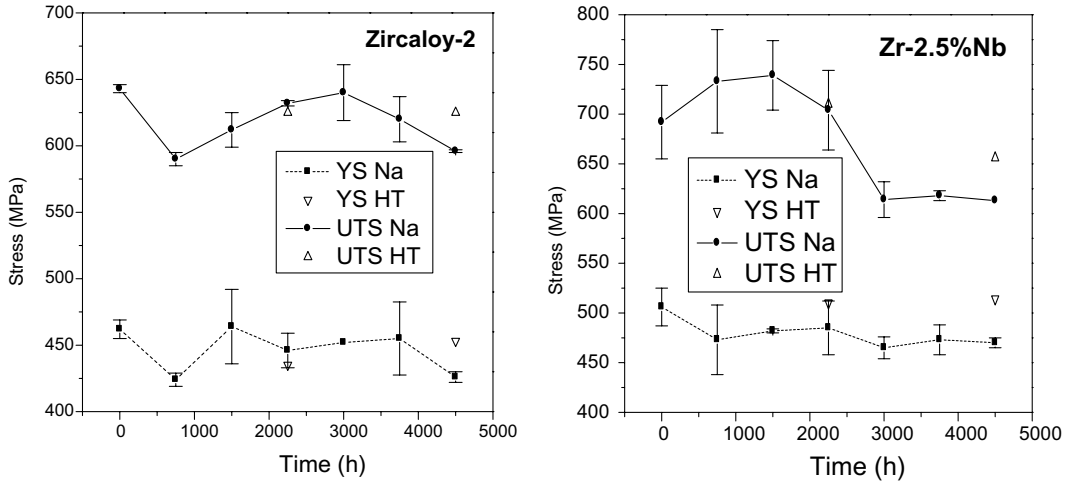

Fig. 6. Effect of exposure to sodium (Na) and thermal aging (HT) at 613 K on yield strength (YS) and ultimate tensile strength (UTS) of Zircaloy-2 and Zr–2.5%Nb alloys.

to unexposed specimens. The ultimate tensile strength was found to increase by a maximum of 7% due to exposure to sodium up to 2250 h and later it was found to decrease by a maximum of 11%. The total elongation was observed to lie between 14.0% and 20.7% for the exposed specimens as compared to 13.6% for unexposed specimens. Microhardness values indicate that the change in the hardness is similar to the change in the ultimate tensile strength.

The SEM fractographs of Zircaloy-2 and Zr–2.5%Nb alloy in sodium exposed conditions (4500 h) are shown in Fig. 8(a) and (b), respectively. The SEM fractographs of Zircaloy-2 and Zr–2.5%Nb alloy in the thermally treated condition are shown in Fig. 8(c) and (d). The fracture is of ductile dimple type in unexposed specimens of the two alloys. Whereas in sodium exposed and thermally treated specimens of the two alloys, microcracking in circumferential direction (Fig. 8(a)–(c)) can

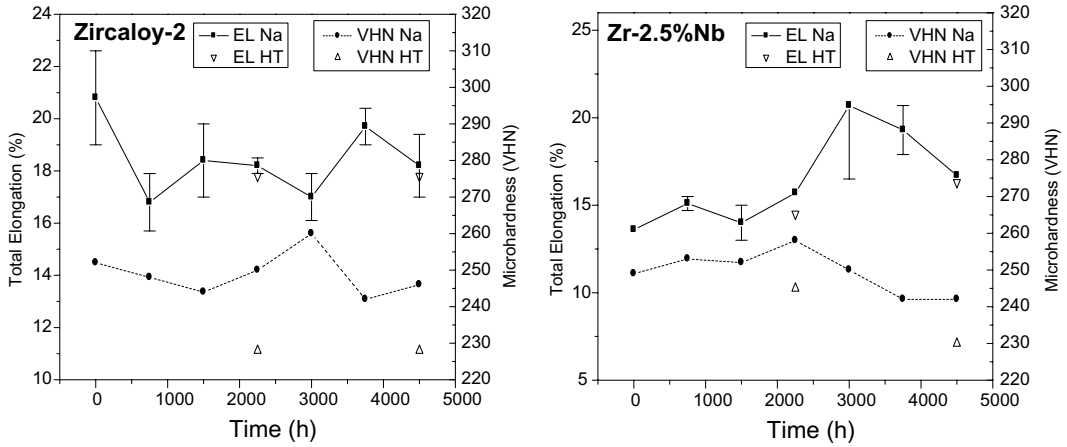

Fig. 7. Effect of exposure to sodium (Na) and thermal aging (HT) at 613 K on (%) total elongation (EL) and microhardness (VHN) of Zircaloy-2 and Zr–2.5%Nb alloys.

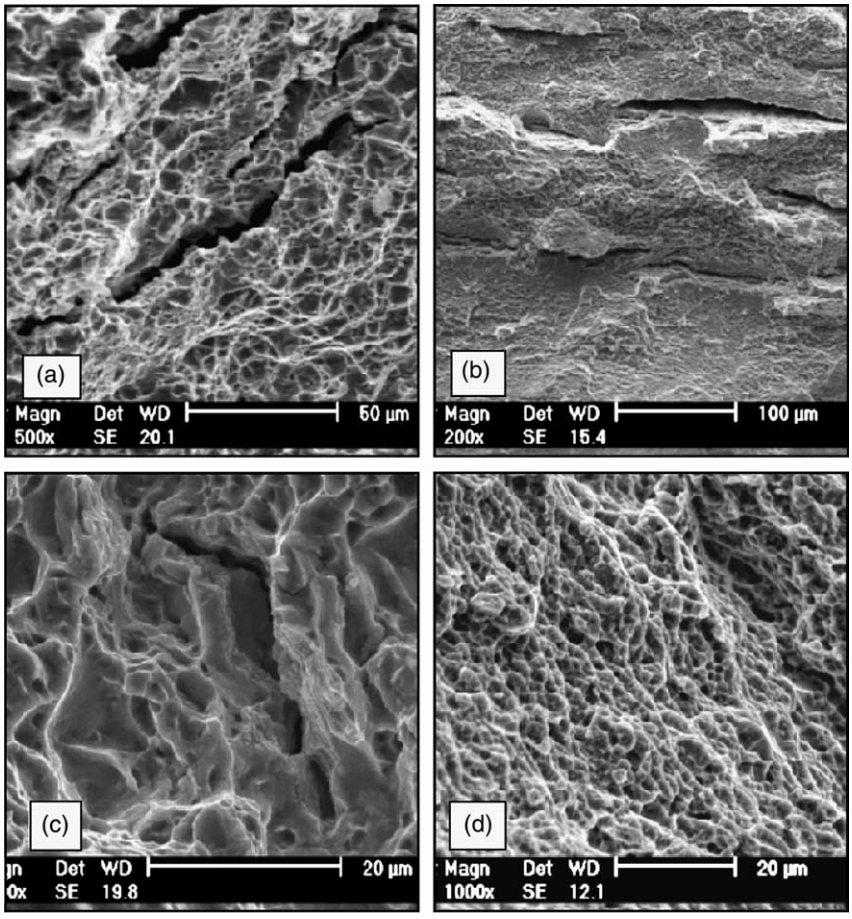

Fig. 8. SEM fractographs of Zircaloy-2 and Zr–2.5%Nb alloys: (a) Zircaloy-2, exposed to sodium for 4500 h; (b) Zr–2.5%Nb, exposed to sodium for 4500 h; (c) Zircaloy-2, thermally aged for 4500 h; (d) Zr–2.5%Nb, thermally aged for 4500 h.

be observed in addition to the ductile dimple fracture. More microcracks can be seen in the sodium exposed specimens as compared to the thermally treated specimens which had less hydrides.

Fig. 9(a)–(c) shows the variation of nominal stress and AE counts with nominal strain of Zircaloy-2 for different durations of exposure to sodium. Fig. 9(d)–(f) shows the variation of nominal stress and AE counts with nominal strain of Zr–2.5%Nb alloy for different durations of exposure to sodium. The total counts generated up to macroyielding, i.e. 0.2% offset yield strength (N_y), and the counts generated between macroyielding and ultimate tensile strength (N_p) of the two alloys for different conditions were determined and are given in Table 5. Fig. 9 and Table 5 indicate that for both these alloys and for both types of treatment, significant AE activity occurs in the region prior to and during yielding. Beyond this, AE generated in both the alloys is reduced. The magnitude of this plastic strain varies depending on the type of alloy and the duration of exposure to sodium. In Zircaloy-2, AE generated in the yield region is reduced in the heat-treated and sodium exposed specimens compared to that in the unexposed specimens. But in Zr–2.5%Nb alloy, the above reduction is marginal. In both the alloys, AE generated in the post-yield region is higher for the specimens exposed to sodium and for those given the thermal treatment as compared to that generated in the non-heat-treated specimens.

5. Discussion

The optical micrographs shown in Figs. 3–5 indicate that the number and the size of the hydride platelets are higher for the sodium exposed specimens as compared to the thermally treated specimens. This can be explained in the following manner. At the cold-trap temperature of 393 K in the sodium loop, where the specimens were exposed to sodium, the impurity level of hydrogen was 0.063 ppm. But the specimens for thermal aging were

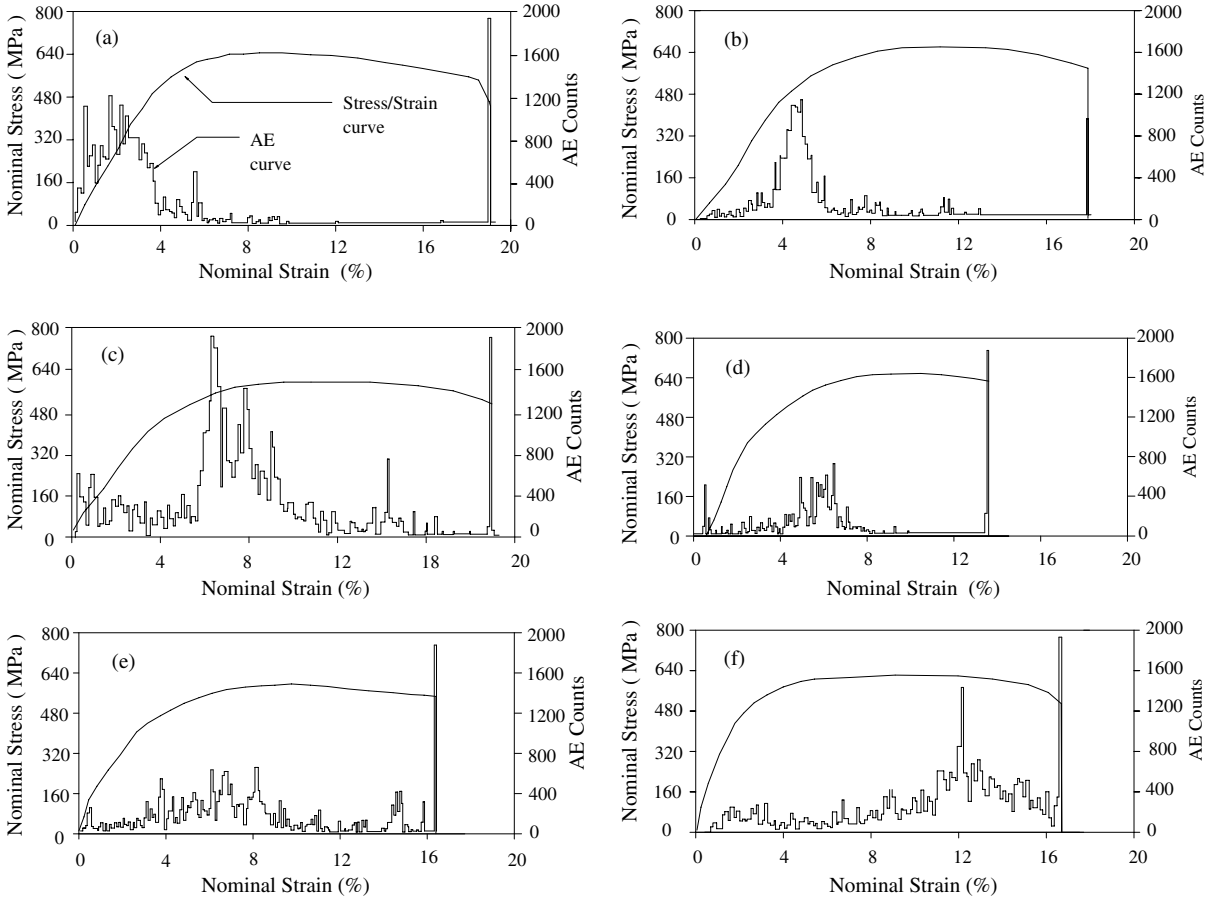

Fig. 9. Variation of nominal stress and AE counts with nominal strain of Zircaloy-2: (a) unexposed condition (0 h), (b) exposed to sodium for 3000 h, (c) exposed to sodium for 3000 h; and Zr–2.5%Nb: (d) unexposed condition (0 h), (e) exposed to sodium for 3000 h, (f) exposed to sodium for 4500 h.

Table 5
Total AE counts up to macroyielding i.e. 0.2% offset yield strength (N_y) and AE counts generated between macroyielding and ultimate tensile strength (N_p)

Duration of exposure to sodium (h)	N_y		N_p	
	Zircaloy-2	Zr–2.5%Nb	Zircaloy-2	Zr–2.5%Nb
Unexposed (0 h)	13 000–19 000	2400–3500	4000–7000	6500–9000
750	5500–9000	1700–2400	9000–13 000	8000–11 000
1500	6000–9000	1600–2200	10 000–15 000	7000–10 000
2250	3500–7000	1700–2400	8000–14 000	9000–17 000
3000	4000–7500	1900–3000	10 000–17 000	11 000–19 000
3750	7000–12 000	1800–2800	16 000–24 000	10 000–15 000
4500	6000–9000	1600–2900	27 000–38 000	15 000–22 000
Thermally aged for 2250 h	7500–12 000	1800–3600	13 000–22 000	6000–11 000
Thermally aged for 4500 h	9500–14 000	1900–3800	25 000–33 000	5000–9000

Data range indicates for different specimens of same condition.

encapsulated in quartz tubes with low pressure argon environment and subjected to a temperature of 613 K in an electrical furnace and hence the availability of hydrogen during thermal exposure was negligible. Although zirconium is a good getter, at the test temperature, the diffusion rate is low and hence hydrogen is absorbed by the specimens exposed in sodium over a period of time. This leads to the formation of more hydrides in sodium exposed specimens as compared to thermally treated specimens.

The tensile results of the two alloys indicate that the significant changes in tensile properties occur for the sodium exposed and thermally treated specimens of Zr–2.5%Nb alloy where the ultimate tensile strength and elongation values show some changes for times >2250 h. This can be attributed to the microstructural alterations in this alloy with exposure/heat treatment time. The microstructure produced after β-quenching of Zr-base alloys contains acicular plates of α-martensite (hcp). In Zr–2.5%Nb alloy, hot-extrusion and pilgering develops a two-phase structure of strongly textured elongated α-grains with high dislocation density and grain boundary network of β-Zr phase [7,8]. Age hardening studies of cold-rolled sheet [9] as well as hot-rolled bar and extruded tube of Zr–2.5%Nb alloy showed [10] that the observed phenomenon at aging temperatures 573–773 K is a competition between hardening by a Nb rich phase and softening by recovery of cold work. It was reported that aging of hot-extruded and cold-drawn Zr–2.5%Nb alloy at 573 and 673 K increases the hardness of the alloy and causes decomposition of β-Zr into ω-phase and β-enriched in Nb at aging times of 3000 and 300 h, respectively [10]. The observed changes in the tensile properties of Zr–2.5%Nb alloy with time can thus be attributed to the occurrence of hardening due to the decomposition of β-phase and coarsening of α-grains.

Comparison of the tensile properties and microhardness of thermally treated specimens of the two alloys (Table 4) with those of sodium exposed specimens indicate that the maximum difference between the values is within 10% and thus, can be considered to be almost similar. These results indicate that the marginal changes in the tensile properties and hardness of the two alloys are essentially due to the thermal effect with almost no effect due to exposure to sodium.

The AE results obtained in this investigation are in agreement with the normally observed AE activity during tensile deformation of metallic materials having essentially a single-phase microstructure that is known to give rise to a peak in AE at initial strain levels corresponding to the phenomenon of macroyielding [3,4]. Both slip and twinning give rise to significant contribution to the deformation of hcp metals. The phenomenological description of AE generation from slip in metals and alloys is that dislocations give rise to AE only if many dislocations move simultaneously within a small volume of the material [3–5]. The avalanche of dislocations must move far and fast enough, otherwise their motion will remain undetected. As deformation proceeds, more and more obstacles reduce the distance that the dislocations move and thereby reduce the size of the elastic waves produced until most of them become undetectable. In materials with hcp structures, in addition to slip, twinning occurs and this is also a potential source of AE during deformation of zirconium alloys [5]. The twinning process occurs in three stages: nucleation of a twin embryo, rapid growth of the embryo into a macroscopically observable twin and thickening of the twin normal to its original growth direction. Regardless of the mechanism by which twinning occurs, the rapid shear deformation from growth of a deformation twin makes it a potent source of AE [4]. AE generation during twin formation in zirconium by indenting the surface with a microhardness indentor was studied and it was reported that one twin produces one AE burst [6]. Tensile testing of zirconium alloys showed one peak in AE in the elastic region, a slight decrease and then another peak at approximately 3% strain, after which AE rapidly falls to zero [2].

The AE generated during tensile deformation of Zircaloy-2 and Zr–2.5%Nb alloy used in the present investigation (in the as-received condition) is thus attributed to both slip and twinning processes occurring during deformation. Reduction in AE activity at higher strains is due to the reduced dislocation activity and reduced occurrence of twinning. The amount of AE in the yield region is reduced in the heat treated and sodium exposed specimens of Zircaloy-2 compared to that in the unexposed specimens. The higher AE generated in the yield region of unexposed specimens compared to thermally treated and exposed specimens is attributed to precipitation of hydride platelets in thermally aged and exposed specimens that reduce the mean free path for dislocation movement and also restricts the extent of dislocation movement. But the AE generated in the yield region for Zr–2.5%Nb alloy is marginally reduced in the heat treated and sodium exposed specimens compared to that in the unexposed specimens. In the heat treated and sodium exposed specimens of Zr–2.5%Nb alloy, coarsening of α-grains takes place thus increasing the glide distance of the dislocations and subsequently increases the AE activity during yielding. The observed marginal reduction in AE in the heat treated and sodium exposed specimens compared to the unexposed specimens of Zr–2.5%Nb alloy can therefore be attributed to the balancing effects of reduction in the mean free path for dislocation movement by precipitation of hydride platelets and increase in the mean free path for dislocation movement due to coarsening of the α-grains.

On the other hand, AE generated in the post-yield region is higher for the thermally treated and sodium exposed specimens as compared to that in the non-heat-treated specimens and extends in the higher strain regions, particularly for time >2250 h. This can be attributed to the decohesion of hydride platelets present in the specimens leading to the nucleation and growth of microcracks during tensile deformation. The presence of hydrides in the sodium exposed and thermally treated specimens as compared to the unexposed specimens of the two alloys is supported by metallographic (Figs. 3–5) results. The occurrence of decohesion and/or fracture of hydride platelets during tensile deformation is supported by the results of fractographic (Fig. 8) examinations. The microcracks observed in different specimens are inferred to correspond to the hydride platelets observed by metallography. This can be further supported by comparing the AE results from specimens exposed to sodium and equivalent thermal treatment. Such results of Zircaloy-2 and Zr–2.5%Nb alloy indicate that AE generated in the post-yield region is higher for the specimens exposed to sodium in both alloys as compared to the thermally treated specimens (Table 5) and this is attributed to more decohesion and/or fracture events in the specimens exposed to sodium. Although the decohesion and/or fracture events are more in the specimens exposed to sodium, the tensile properties of both types of specimens are almost similar. Hence, such small differences could be advantageously brought out by AE monitoring during tensile deformation, demonstrating the sensitivity and hence the potential of AET for studying dynamic events and to gain more insight into deformation aspects.

It is known [11] that the fracture strength of hydrides during tensile deformation is a sensitive function of the length of the hydride platelets. It is also known [12] that a higher stress is needed for decohesion/fracture of small hydrides and essentially no plastic strain is needed for decohesion/fracture of large hydrides. Thus, depending on the variations in the internal stress of hydride platelets and the hydride aspect ratio, the decohesion and/or fracture of hydride platelets could occur over a range of applied stress and this could influence the generation of AE activity [11]. The variation in AE activity among different heat-treated and sodium exposed specimens can thus be attributed to the variation in the size, number density and internal stresses around the hydride platelets. The generation of AE due to decohesion and/or fracture of hydrides has been reported in the literature [12–14]. The study of AE during tensile deformation of cold-worked Zr–2.5%Nb alloy showed that a rapid and continuous increase in the AE event rate was coincided with the initiation of hydride cracking as compared to the lower event rate during the early stage of the deformation [13]. AE studies during tensile deformation of Zr–2.5%Nb alloy were also reported [14] where the generation of higher acoustic activity from samples containing hydrides as compared to non-hydrided samples was observed. It was shown that AE events from both types of samples were of similar amplitude. The higher AE in the hydrided sample in the post-yield region as compared to lower AE in the non-hydrided sample was attributed to the fracture of hydride platelets occurring during tensile deformation [14]. The results from the present study are in agreement with the above discussed results obtained by various investigators. These specific differences in amount of hydrides and extent of decohesion could not be reflected in tensile properties but could be brought out by AE analysis.

6. Conclusion

The compatibility of Zircaloy-2 and Zr–2.5%Nb alloys with sodium up to the temperature of 613 K has been established. The changes in strength and ductility for both alloys due to either thermal treatment or exposure to sodium were found to be very marginal and almost similar. The AE generated during yielding of all the specimens is attributed to slip and twinning processes in these alloys. In Zircaloy-2, lower AE during yielding in thermally treated and sodium exposed specimens as

compared to unexposed specimens has been attributed to reduced dislocation mean free path consequent to precipitation of hydride platelets. The marginal reduction in AE in the heat treated and sodium exposed specimens of Zr–2.5%Nb alloy as compared to the unexposed specimens has been attributed to the balancing effects of reduction in the mean free path for dislocation movement by formation of hydride platelets and increase in the mean free path for dislocations due to coarsening of α-grains. The AE generated at higher strain regions in the thermally treated and sodium exposed specimens of both the alloys is attributed to decohesion and fracture of hydride platelets and has been supported by metallographic and fractographic observations.

Acknowledgements

The support and encouragement received from Dr Baldev Raj, Director, Materials, Chemical & Reprocessing Groups, Indira Gandhi Centre for Atomic Research (IGCAR), Kalpakkam, is gratefully acknowledged. The help received from staff members of Metallurgy and Chemical Groups of IGCAR, in carrying out this work is also thankfully acknowledged.

References

[1] R.N. Lyon, Liquid Metals Handbook, Oak Ridge National Laboratory, Oak Ridge, TN, 1952.
[2] P. McIntire, Nondestructive Testing Handbook, Acoustic Emission Testing, vol. 5, American Society for Nondestructive Testing, 1987.
[3] H. Imeda, K. Kuganagi, H. Kimura, H. Nakasa, in: Proceedings of the Third Acoustic Emission Symposium, Tokyo, Japan, 1976, p. 492.
[4] C.R. Heiple, S.H. Carpenter, J. Acoust. Emiss. 6 (1987) 177.
[5] C.R. Heiple, S.H. Carpenter, J. Acoust. Emiss. 6 (1987) 215.
[6] V.S. Boiko, L.G. Ivanchenko, L.F. Krivenko, Sov. Phys. Solid State 26 (1984) 1340.
[7] B.A. Cheadle, C.E. Ells, W. Evans, J. Nucl. Mater. 23 (1967) 199.
[8] B.A. Cheadle, S.A. Aldrige, C.E. Ells, Can. Metall. Q. 11 (1972) 121.
[9] C.E. Ells, B.A. Cheadle, J. Nucl. Mater. 23 (1967) 257.
[10] S.A. Aldrige, B.A. Cheadle, J. Nucl. Mater. 42 (1972) 32.
[11] S.Q. Shi, M.P. Puls, J. Nucl. Mater. 275 (1999) 312.
[12] M.P. Puls, Metall. Trans. 19A (1988) 1507.
[13] R. Choubey, M.P. Puls, Metall. Mater. Trans. 25A (1994) 993.
[14] T. Chow, D.A. Hutchins, M.D.C. Moles, R.P. Young, Ultrasonics 31 (1993) 183.